

Electronic Supplementary Information for
**Triple-Layered PPy@NiCo LDH/FeCo₂O₄ Hybrid Structure with High Electron
Conductivity and Abundant Interfaces for Supercapacitor and Oxygen
Evolution**

*Jing He,^a Zhufeng Hu,^a Kuan Deng,^a Renjun Zhao,^a Xingbin Lv,^a Wen Tian,^a Yu Xin
Zhang,^b Junyi Ji^{a, c,*}*

^a School of Chemical Engineering, Sichuan University, Chengdu 610065, P. R. China

^b College of Material Science and Engineering, Chongqing University, Chongqing, 400044, P. R. China.

^c State Key Laboratory of Polymer Materials Engineering, Sichuan University, Chengdu 610065, P. R. China

* Corresponding author.

Junyi Ji, E-mail: junyiji@scu.edu.cn

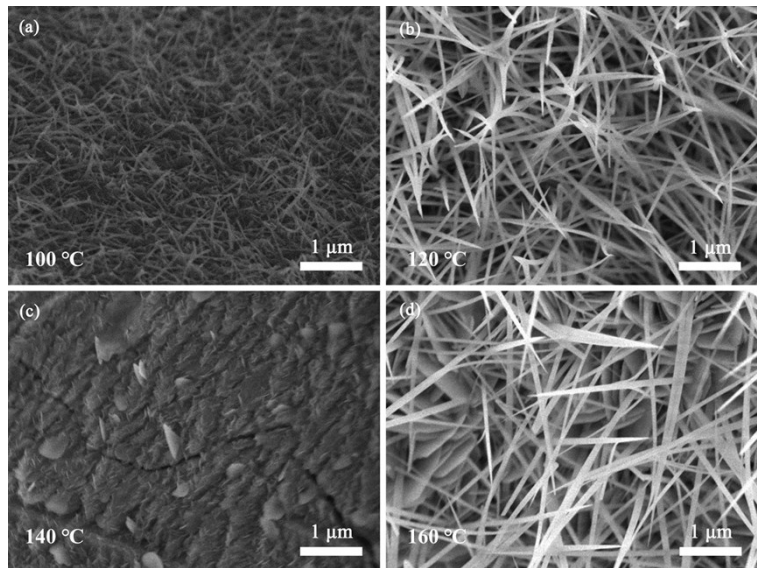


Fig. S1 SEM images of the NiFeCo/NF composites synthesized under different temperature.

The as-prepared NiFeCo/NF composites synthesized under different temperatures are shown in **Fig. S1**. The lengths of the nanowires tend to increase with the increase of temperature, which may due to the higher crystalline rate. As the loading mass of the composite fabricated at 100 °C is relatively low, while the hybrid prepared at 160 °C reveals a nanosheets/nanowire mix morphology. Moreover, the energy storage performance of the manufactured at 120 °C is significantly superior than other composites (**Fig. S2**), therefore, the temperature of 120 °C is chosen for further research.

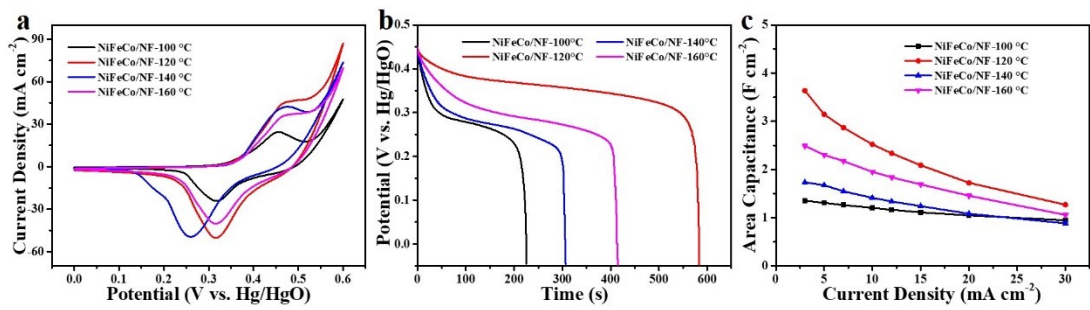


Fig. S2 a) CV curves, b) charge-discharge curves, and c) rate performance of the NiFeCo/NF composites prepared under different temperature.

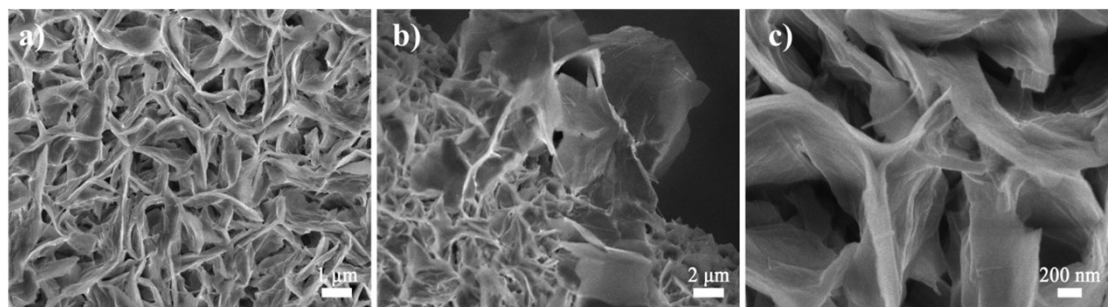


Fig. S3 SEM images of the PPy@NiFeCo/NF-4 electrode at different magnification.

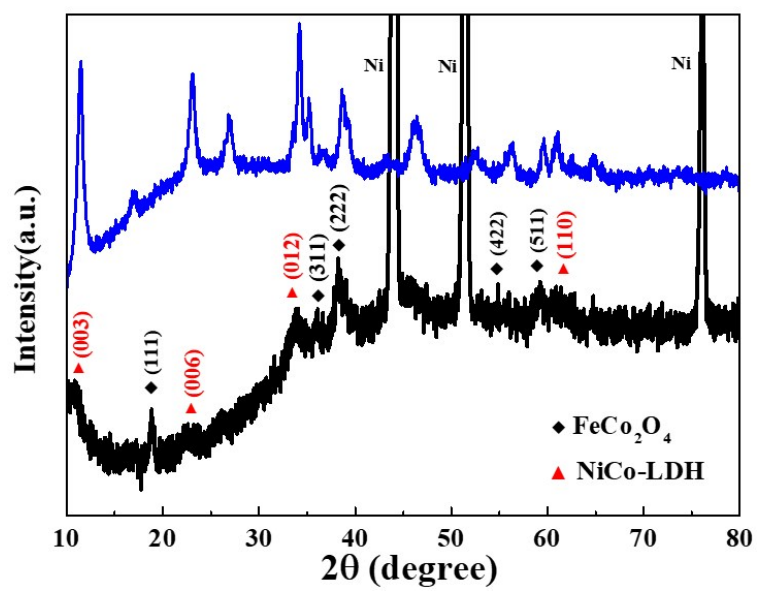


Fig. S4 XRD pattern of the NiFeCo/NF and the NiFeCo powder.

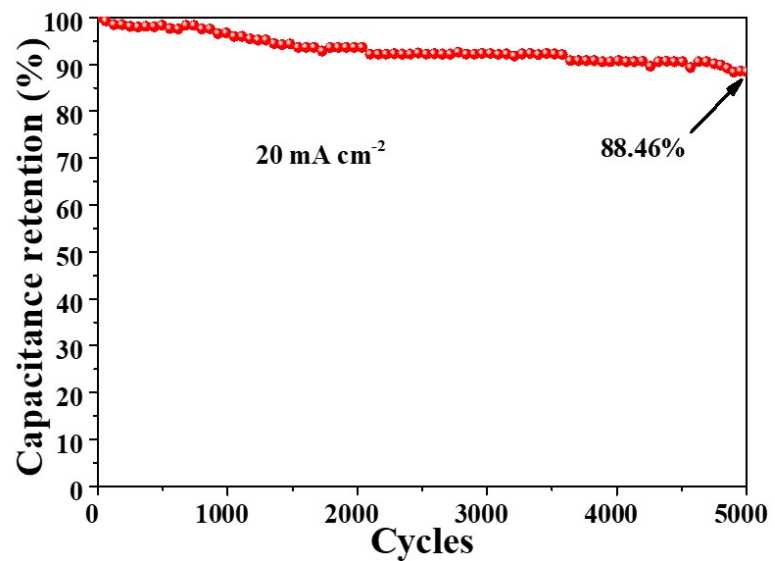


Fig. S5 Long-term cycling stability of the PPy@NiCo-LDH@FeCo₂O₄-4.

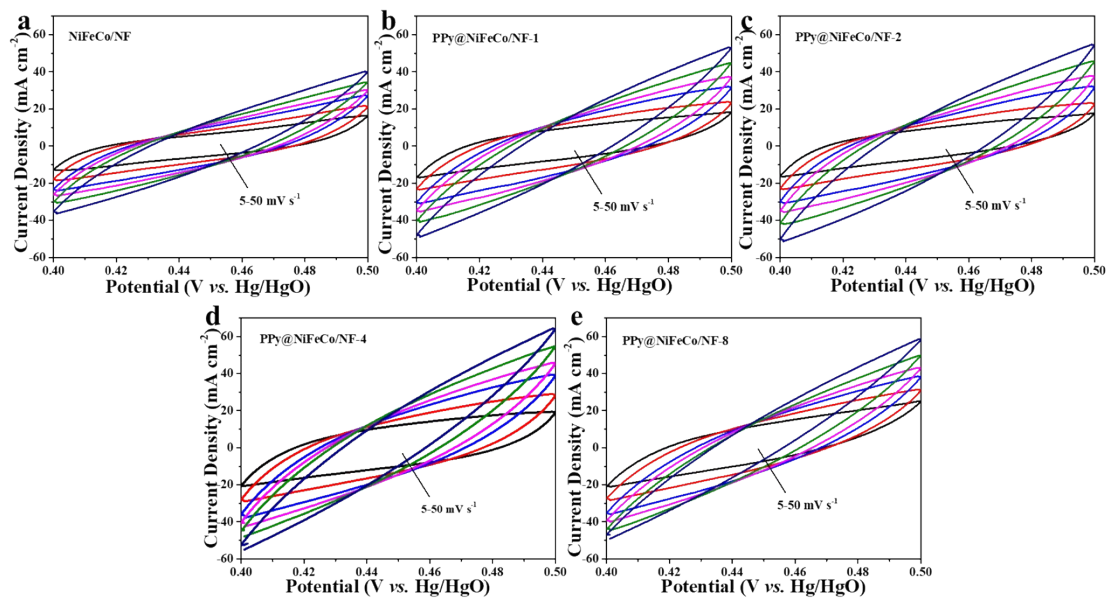


Fig. S6 CV curves of the NiFeCo/NF and PPy@NiFeCo/NF-n at different scan rates for the calculation of C_{dl} values.

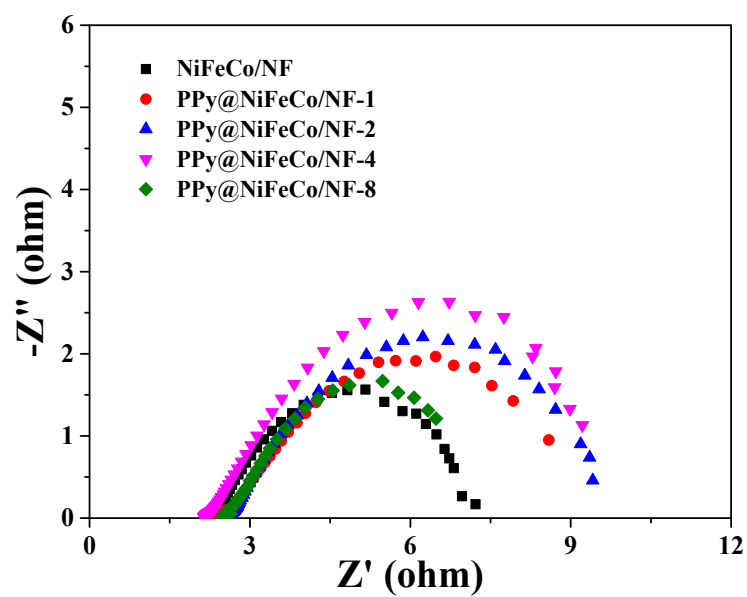


Fig. S7 Electrochemical impedance spectra tested in electrocatalyst at onset overpotential.

Table. S1 Inductively coupled plasma mass spectrometry results of NiCo-LDH@FeCo₂O₄.

Element	Fe	Co
Content (%)	1.26	5.47

Table S2. Comparison of the specific capacitance of some related metallic composite in previous reports.

Materials	Specific Capacitance	Reference
CoS ₂ /MoS ₂ nanosheet	605.77 mF cm ⁻² (1.0 mA cm ⁻²)	1
P-Doped NiCo ₂ S ₄ nanotubes	8.03 F cm ⁻² (2 mA cm ⁻²)	2
Ni ₃ S ₂ /NF	5.633 F cm ⁻² (10 mA cm ⁻²)	3
NiCo ₂ S ₄ @Ni(OH) ₂ @PPy	9.1125 F cm ⁻² (5 mA cm ⁻²)	4
NiV LDHs@P-NF	2.85 F cm ⁻² (20 mA cm ⁻²)	5
V ₅ O ₁₂ /VO ₂	5.03 F cm ⁻² (1 mA cm ⁻²)	6
CoO/NiO-Cu@CuO	2.035 F cm ⁻² (2 mA cm ⁻²)	7
Co(OH) ₂ /CoOOH/Co ₃ O ₄ /Cu(OH) ₂	1.94 F cm ⁻² (1 mA cm ⁻²)	8
MnCo ₂ O ₄ @NiWO ₄	5.09 F cm ⁻² (1 mA cm ⁻²)	9
graded holey NiCo LDH	9.03 F cm ⁻² (1 mA cm ⁻²)	10
This work	9.24 F cm ⁻² (5 mA cm ⁻²)	

Table S3. The specific resistance value of EIS fitting results in supercapacitor tests.

	R _s (Ω)	R ₁ (Ω)	R ₂ (Ω)	W _s (Ω)
NiFeCo/NF	0.75	1.67	1.70	11.4
PPy@NiFeCo/NF-1	0.53	1.30	1.42	10.8
PPy@NiFeCo/NF-2	0.42	0.67	1.68	9.2
PPy@NiFeCo/NF-4	0.56	0.70	1.11	8.6
PPy@NiFeCo/NF-8	0.61	1.30	1.44	11.1

Table S4. Comparison of overpotential and their corresponding Tafel slope of related electrodes for OER in previous reports.

Materials	Overpotential for OER	Tafel Slope	Reference
CoS ₂ -MoS ₂	266 mV (10 mA cm ⁻²)	59 mV dec ⁻¹	11
NiFeBRu	245 mV (10 mA cm ⁻²)	15 mV dec ⁻¹	12
NiFe LDH	243 mV (10 mA cm ⁻²)	50 mV dec ⁻¹	13
Fe ₃ N	285 mV (10 mA cm ⁻²)	34 mV dec ⁻¹	14
NiFeCo-LDH/CF	249 mV (10 mA cm ⁻²)	42 mV dec ⁻¹	15
FeNi ₃ N-Ni ₃ S ₂	230 mV (10 mA cm ⁻²)	38 mV dec ⁻¹	16
CoNi-S/NS-rGO	290 mV (10 mA cm ⁻²)	79.5 mV dec ⁻¹	17
Ni ₃ S ₂ /CoFe ₂ O ₄	254 mV (50 mA cm ⁻²)	54.4 mV dec ⁻¹	18
This work	244 mV (50 mA cm ⁻²)	64.39 mV dec ⁻¹	

Reference

- Y. Xie and Y. Wang, *Electrochim. Acta*, 2020, 137224.
- J. Lin, Y. Wang, X. Zheng, H. Liang, H. Jia, J. Qi, J. Cao, J. Tu, W. Fei and J. Feng, *Dalt. Trans.*, 2018, 47, 8771-8778.
- L. Chen, J. Zeng, M. Guo, R. Xue, R. Deng and Q. Zhang, *J. Colloid Interf. Sci.*, 2021, 583, 594-604.
- M. Liang, M. Zhao, H. Wang, J. Shen and X. Song, *J. Mater. Chem. A*, 2018, 6, 2482-2493.
- G. Wang, Z. Jin and Q. Guo, *J. Colloid Interf. Sci.*, 2021, 583, 1-12.
- R. Dong, Y. Song, D. Yang, H.-Y. Shi, Z. Qin, M. Zhang, D. Guo, X. Sun and X.-X. Liu, *J. Mater. Chem. A*, 2020, 8, 1176-1183.
- A. Zhang, L. Yue, D. Jia, L. Cui, D. Wei, W. Huang, R. Liu, Y. Liu, W. Yang and J. Liu, *ACS Appl. Mater. Interfaces*, 2020, 12, 2591-2600.
- Y. Yu, H. Wang, H. Zhang, Y. Tan, Y. Wang, K. Song, B. Yang, L. Yuan, X. Shen and X. Hu, *Electrochim. Acta*, 2020, 334, 135559.
- X. Guo, M. Li, Y. Liu, Y. Huang, S. Geng, W. Yang and Y. Yu, *J. Colloid Interf. Sci.*, 2020, 563, 405-413.
- T. Yang, Q. Ye, Y. Liang, L. Wu, X. Long, X. Xu and F. Wang, *J. Power Sources*, 2020, 449, 227590.
- Y. Li, W. Wang, B. Huang, Z. Mao, R. Wang, B. He, Y. Gong and H. Wang, *J. Energy Chem.*, 2021, 57, 99-108.
- G. Xi, L. Zuo, X. Li, Y. Jin, R. Li and T. Zhang, *J. Mater. Sci. Technol.*, 2021, 70, 197-204.
- C. Wu, H. Li, Z. Xia, X. Zhang, R. Deng, S. Wang and G. Sun, *ACS Catal.*, 2020,

- 10, 11127–11135.
- 14. J. Dong, Y. Lu, X. Tian, F.-Q. Zhang, S. Chen, W. Yan, H.-L. He, Y. Wang, Y.-B. Zhang, Y. Qin, M. Sui, X.-M. Zhang and X. Fan, *Small*, 2020, 2003824.
 - 15. Y. Lin, H. Wang, C.-K. Peng, L. Bu, C.-L. Chiang, K. Tian, Y. Zhao, J. Zhao, Y.-G. Lin, J.-M. Lee and L. Gao, *Small*, 2020, 2002426.
 - 16. S. Liang, M. Jing, E. Pervaiz, H. Guo, T. Thomas, W. Song, J. Xu, A. Saad, J. Wang, H. Shen, J. Liu and M. Yang, *ACS Appl. Mater. Interfaces*, 2020, 12, 41464–41470
 - 17. M. B. Zakaria, D. Zheng, U.-p. Apfel, T. Nagata, E.-R. S. Kenawy and J. Lin, *ACS Appl. Mater. Interfaces*, 2020, 12, 40186-40193.
 - 18. J.-J. Duan, R.-L. Zhang, J.-J. Feng, L. Zhang, Q.-L. Zhang and A.-J. Wang, *J. Colloid Interf. Sci.*, 2021, 581, 774-782.